

Off-shell Higgs Couplings in $H^* \rightarrow ZZ \rightarrow \ell\nu\nu$

Dorival Gonçalves

Department of Physics, Oklahoma State University, Stillwater, OK, 74078, USA

Tao Han, Sze Ching Iris Leung, and Han Qin

*PITT PACC, Department of Physics and Astronomy,
University of Pittsburgh, 3941 O'Hara St., Pittsburgh, PA 15260, USA*

We explore the new physics reach for the off-shell Higgs boson measurement in the $pp \rightarrow H^* \rightarrow Z(\ell^+\ell^-)Z(\nu\bar{\nu})$ channel at the high-luminosity LHC. The new physics sensitivity is parametrized in terms of the Higgs boson width, effective field theory framework, and a non-local Higgs-top coupling form factor. Adopting Machine-learning techniques, we demonstrate that the combination of a large signal rate and a precise phenomenological probe for the process energy scale, due to the transverse ZZ mass, leads to significant sensitivities beyond the existing results in the literature for the new physics scenarios considered.

I. INTRODUCTION

After the Higgs boson discovery at the Large Hadron Collider (LHC) [1–5], the study of the Higgs properties has been one of the top priorities in searching for new physics beyond the Standard Model (BSM). Indeed, the Higgs boson is a unique class in the SM particle spectrum and is most mysterious in many aspects. The puzzles associated with the Higgs boson include the mass hierarchy between the unprotected electroweak (EW) scale (v) and the Planck scale (M_{PL}), the neutrino mass generation, the possible connection to dark matter, the nature of the electroweak phase transition in the early universe, to name a few. Precision studies of the Higgs boson properties can be sensitive to new physics at a higher scale. Parametrically, new physics at a scale Λ may result in the effects of the order v^2/Λ^2 .

So far, the measurements at the LHC based on the Higgs signal strength are in full agreement with the SM predictions. However, these measurements mostly focus on the on-shell Higgs boson production, exploring the Higgs properties at low energy scales of the order v . It has been argued that if we explore the Higgs physics at a higher scale Q , the sensitivity can be enhanced as Q^2/Λ^2 . A particularly interesting option is to examine the Higgs sector across different energy scales, using the sizable off-shell Higgs boson rates at the LHC [6–10]. While the off-shell Higgs new physics sensitivity is typically derived at the LHC with the $H^* \rightarrow ZZ \rightarrow 4\ell$ channel [11–18], we demonstrate in this work that the extension to the channel $ZZ \rightarrow \ell\nu\nu$ can significantly contribute to the potential discoveries. This channel provides two key ingredients to probe the high energy regime with enough statistics despite of the presence of two missing neutrinos in the final state. First, it displays a larger event rate by a factor of six than the four charged lepton channel. Second, the transverse mass for the ZZ system sets the physical scale Q^2 and results in a precise phenomenological probe to the underlying physics.

In this paper, we extend the existing studies and carry out comprehensive analyses for an off-shell channel in the

Higgs decay

$$pp \rightarrow H^* \rightarrow ZZ \rightarrow \ell^+\ell^- \nu\bar{\nu}, \quad (1)$$

where $\ell = e, \mu$ and $\nu = \nu_e, \nu_\mu, \nu_\tau$. Because of the rather clean decay modes, we focus on the leading production channel of the Higgs boson via the gluon fusion. First, we phenomenologically explore a theoretical scenario with additional unobserved Higgs decay channels leading to an increase in the Higgs boson width, $\Gamma_H/\Gamma_H^{SM} > 1$. The distinctive dependence for the on-shell and off-shell cross-sections with the Higgs boson width foster the conditions for a precise measurement for this key ingredient of the Higgs sector. We adopt the Machine-learning techniques in the form of Boosted Decision Tree (BDT) to enhance the signal sensitivity. This analysis sets the stage for our followup explorations. Second, we study the effective field theory framework, taking advantage of the characteristic energy-dependence from some of the operators. Finally, we address a more general hypothesis that features a non-local momentum-dependent Higgs-top interaction [18], namely, a form factor, that generically represents the composite substructure. Overall, the purpose of this paper is to highlight the complementarity across a multitude of frameworks [13–19] via the promising process at the LHC $H^* \rightarrow Z(\ell\ell)Z(\nu\nu)$, from models that predict invisible Higgs decays, passing by the effective field theory, and a non-local form-factor scenario. Our results demonstrate significant sensitivities at the High-Luminosity LHC (HL-LHC) to the new physics scenarios considered here beyond the existing literature.

The rest of the paper is organized as follows. In Sec. II, we derive the Higgs width limit at HL-LHC. Next, in Sec. III, we study the new physics sensitivity within effective field theory framework. In Sec. IV, we scrutinize the effects of a non-local Higgs-top form-factor. Finally, we present a summary in Sec. V.

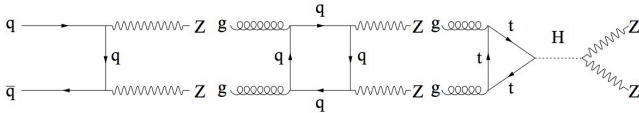


Figure 1. Representative Feynman diagrams for the DY $q\bar{q} \rightarrow ZZ$ (left), GF $gg \rightarrow ZZ$ continuum (center), and s -channel Higgs signal $gg \rightarrow H^* \rightarrow ZZ$ (right).

II. HIGGS BOSON WIDTH

The combination of on-shell and off-shell Higgs boson rates addresses one of the major shortcomings of the LHC, namely the Higgs boson width measurement [6, 7]. This method breaks the degeneracy present on the on-shell Higgs coupling studies

$$\sigma_{i \rightarrow H \rightarrow f}^{\text{on-shell}} \propto \frac{g_i^2(m_H)g_f^2(m_H)}{\Gamma_H}, \quad (2)$$

where the total on-shell rate can be kept constant under the transformation $g_{i,f}(m_H) \rightarrow \xi g_{i,f}(m_H)$ with $\Gamma_H \rightarrow \xi^4 \Gamma_H$. The off-shell Higgs rate, due to a sub-leading dependence on the Higgs boson width Γ_H

$$\sigma_{i \rightarrow H^* \rightarrow f}^{\text{off-shell}} \propto g_i^2(\sqrt{\hat{s}})g_f^2(\sqrt{\hat{s}}), \quad (3)$$

breaks this degeneracy, where $\sqrt{\hat{s}}$ is the partonic c.m. energy that characterizes the scale of the off-shell Higgs. In particular, if the new physics effects result in the same coupling modifiers at both kinematical regimes [13–16], the relative measurement of the on-shell and off-shell signal strengths can uncover the Higgs boson width, $\mu_{\text{off-shell}}/\mu_{\text{on-shell}} = \Gamma_H/\Gamma_H^{SM}$.

In this section, we derive a projection for the Higgs boson width measurement at the $\sqrt{s} = 14$ TeV high-luminosity LHC, exploring the $ZZ \rightarrow 2\ell 2\nu$ final state. We consider the signal channel as in Eq. (1). The signal is characterized by two same-flavor opposite sign leptons, $\ell = e$ or μ , which reconstruct a Z boson and recoil against a large missing transverse momentum from $Z \rightarrow \nu\bar{\nu}$. The major backgrounds for this search are the Drell-Yan (DY) processes $q\bar{q} \rightarrow ZZ, ZW$ and gluon fusion (GF) $gg \rightarrow ZZ$ process, see Fig. 1 for a sample of the Feynman diagrams. While the Drell-Yan component displays the largest rate, the gluon fusion box diagrams interfere with the Higgs signal, resulting in important contributions mostly at the off-shell Higgs regime [6].

In our calculations, the signal and background samples are generated with MadGraph5_aMC@NLO [20, 21]. The Drell-Yan background is generated at the NLO with the MC@NLO algorithm [22]. Higher order QCD effects to the loop-induced gluon fusion component are included via a universal K -factor [8, 23]. Spin correlation effects for the Z and W bosons decays are obtained in our simulations with the MADSPIN package [24]. The renormalization and factorization scales are set by the invariant mass of the gauge boson pair $Q = m_{VV}/2$, using the PDF set NN23NLO [25]. Hadronization and underlying event effects are simulated with PYTHIA8 [26], and detector effects are accounted for with the DELPHES3 package [27].

We start our analysis with some basic lepton selections. We require two same-flavor and opposite sign leptons with $|\eta_\ell| < 2.5$ and $p_{T\ell} > 10$ GeV in the invariant mass window $76 \text{ GeV} < m_{\ell\ell} < 106 \text{ GeV}$. To suppress the SM backgrounds, it is required large missing energy selection $E_T^{\text{miss}} > 175 \text{ GeV}$ and a minimum transverse mass for the ZZ system $m_T^{ZZ} > 250 \text{ GeV}$, defined as

$$m_T^{ZZ} = \sqrt{\left(\sqrt{m_Z^2 + p_{T(\ell\ell)}^2} + \sqrt{m_Z^2 + (E_T^{\text{miss}})^2}\right)^2 - \left|\vec{p}_{TZ} + \vec{E}_T^{\text{miss}}\right|^2}. \quad (4)$$

The consistency of our event simulation and analysis setup is confirmed through a cross-check with the ATLAS study in Ref. [9].

To further control the large Drell-Yan background, a Boosted Decision Tree (BDT) is implemented via the Toolkit for Multivariate Data Analysis with ROOT (TMVA) [28]. The BDT is trained to distinguish the full background events from the s -channel Higgs production. The variables used in the BDT are missing transverse energy, the momenta and rapidity for the leading and sub-leading leptons ($p_T^{\ell 1}, \eta^{\ell 1}, p_T^{\ell 2}, \eta^{\ell 2}$), the leading jet ($p_T^{j 1}, \eta^{j 1}$), the separation between the two charged leptons $\Delta R_{\ell\ell}$, the azimuthal angle difference between the di-lepton system and the missing transverse energy $\Delta\phi(\vec{p}_T^{\ell\ell}, \vec{E}_T^{\text{miss}})$, and the scalar sum of jets and lepton

transverse momenta H_T . Finally, we also include the polar θ and azimuthal ϕ angles of the charged lepton ℓ^- in the Z rest frame [29, 30]. We choose the coordinate system for the Z rest frame following Collins and Soper (Collins-Soper frame) [31]. The signal and background distributions for these observables are illustrated in Fig. 2. We observe significant differences between the s -channel signal and background in the (θ, ϕ) angle distributions. These kinematic features arise from the different Z boson polarizations for the signal and background components at the large di-boson invariant mass m_T^{ZZ} [15, 32]. Whereas the s -channel Higgs tends to have Z_L dominance, the DY background is mostly Z_T dominated.

We would like to illustrate the power of the imple-

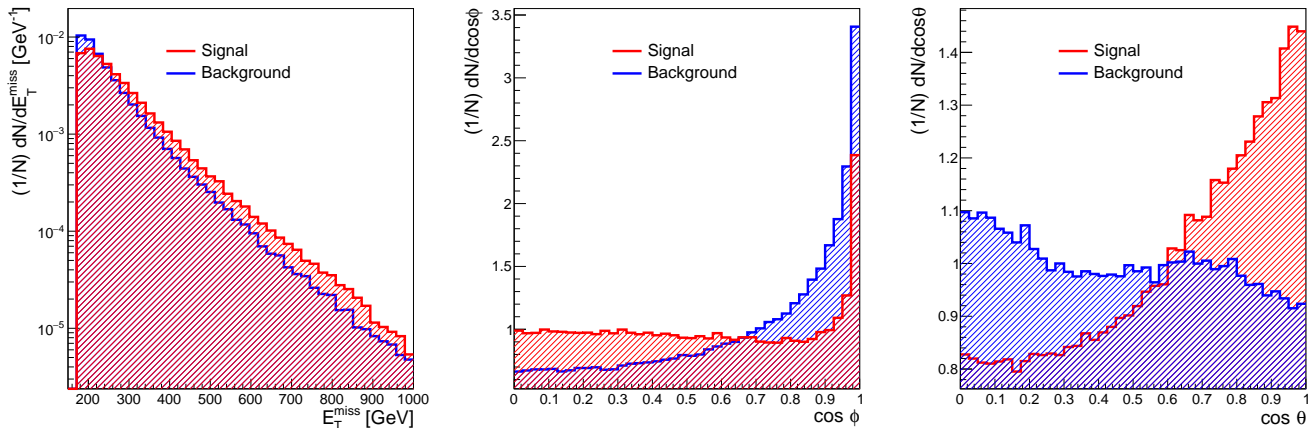


Figure 2. Normalized distributions for the missing transverse momentum E_T^{miss} (left panel), azimuthal ϕ (central panel) and polar θ angles (right panel) of the charged lepton ℓ^- in the Z boson rest frame.

mented BDT analysis to separate the s -channel Higgs from the background contributions in Fig. 3. The BDT discriminator is defined in the range $[-1, 1]$. The events with discriminant close to -1 are classified as background-like and those close to 1 are signal-like. The optimal BDT score selection has been performed with TMVA. To estimate the effectiveness of the BDT treatment, we note that one can reach $S/\sqrt{S+B} = 5$ at an integrated luminosity of 273 fb^{-1} with signal efficiency 88% and background rejection of 34%, by requiring $\text{BDT}_{\text{response}} > -0.26$. Now that we have tamed the dominant backgrounds $q\bar{q} \rightarrow ZZ, ZW$, we move on to the new physics sensitivity study.

To maximize the sensitivity of the Higgs width measurement, we explore the most sensitive variable, m_T^{ZZ} distribution, and perform a binned log-likelihood ratio analysis. In Fig. 4, we display the 95% CL on the Higgs width Γ_H/Γ_H^{SM} as a function of the $\sqrt{s} = 14 \text{ TeV}$ LHC luminosity. To infer the relevance of the multivariate analy-

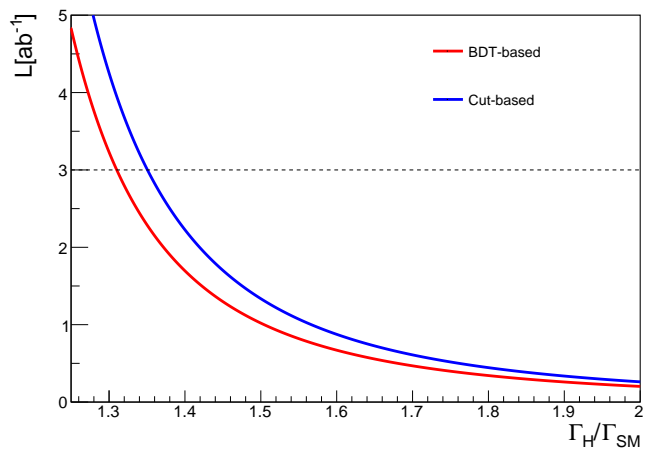


Figure 4. 95% CL bound on the Higgs width Γ_H/Γ_H^{SM} as a function of the $\sqrt{s} = 14 \text{ TeV}$ LHC luminosity. We display the results for the cut-based study (blue) and BDT-based analysis (red).

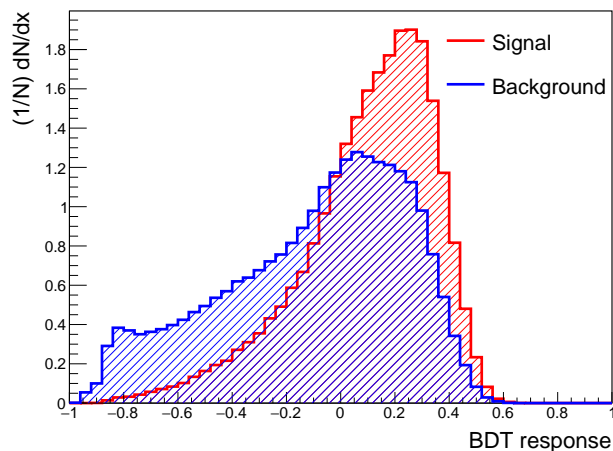


Figure 3. BDT distribution for the s -channel Higgs signal (red) and background (blue).

sis, that particularly explore the observables $(E_T^{\text{miss}}, \theta, \phi)$ depicted in Fig. 2, we display the results in two analysis scenarios: in blue we show the cut-based analysis and in red the results accounting for the BDT-based framework. The significant sensitivity enhancement due to the BDT highlights the importance of accounting for the full kinematic dependence, including the Z -boson spin correlation effects. Whereas the Higgs width can be constrained to $\Gamma_H/\Gamma_H^{SM} < 1.35$ at 95% CL level following the cut-based analysis, $\Gamma_H/\Gamma_H^{SM} < 1.31$ in the BDT-based study assuming $\mathcal{L} = 3 \text{ ab}^{-1}$ of data. Hence, the BDT limits result in an improvement of $\mathcal{O}(5\%)$ on the final Higgs width sensitivity. These results are competitive to the HL-LHC estimates for the four charged lepton final state derived by ATLAS and CMS, where the respective limits are $\Gamma_H/\Gamma_H^{SM} < \mathcal{O}(1.3)$ and $\mathcal{O}(1.5)$ at 68% CL [33, 34].

III. EFFECTIVE FIELD THEORY

The Effective Field Theory (EFT) provides a consistent framework to parametrize beyond the SM effects in the presence of a mass gap between the SM and new physics states. In this context, the new physics states can be integrated out and parametrized in terms of higher dimension operators [35]. In this section we parametrize the new physics effects in terms of the EFT framework [36, 37]. Instead of performing a global coupling fit, we will focus on a relevant subset of higher dimension operators that affect the Higgs production via gluon fusion. This will shed light on the new physics sensitivity for the off-shell $pp \rightarrow H^* \rightarrow Z(\ell\ell)Z(\nu\nu)$ channel. Our effective Lagrangian can be written as

$$\mathcal{L} \supset c_g \frac{\alpha_s}{12\pi v^2} |\mathcal{H}|^2 G_{\mu\nu} G^{\mu\nu} + c_t \frac{y_t}{v^2} |\mathcal{H}|^2 \bar{Q}_L \tilde{\mathcal{H}} t_R + \text{h.c.}, \quad (5)$$

where \mathcal{H} is the SM Higgs doublet and $v = 246$ GeV is the vacuum expectation value of the SM Higgs field. The couplings are normalized in such a way for future convenience. If we wish to make connection with the new physics scale Λ , we would have the scaling as $c_g, c_t \sim v^2/\Lambda^2$. After electroweak symmetry breaking, Eq. (5) renders into the following interaction terms with a single Higgs boson

$$\mathcal{L} \supset \kappa_g \frac{\alpha_s}{12\pi v} H G_{\mu\nu} G^{\mu\nu} - \kappa_t \frac{m_t}{v} H (\bar{t}_R t_L + \text{h.c.}), \quad (6)$$

where the coupling modifiers $\kappa_{g,t}$ and the Wilson coefficients $c_{g,t}$ are related by $\kappa_g = c_g$ and $\kappa_t = 1 - \text{Re}(c_t)$. We depict in Fig. 5 the $gg \rightarrow ZZ$ Feynman diagrams that account for these new physics effects.

Whereas Eq. (5) represents only a sub-set of high dimensional operators affecting the Higgs interactions [36, 37], we focus on it to highlight the effectiveness for the off-shell Higgs measurements to resolve a notorious degeneracy involving these terms. The gluon fusion Higgs production at low energy regime can be well approximated by the Higgs Low Energy Theorem [38, 39], where the total Higgs production cross-section scales as $\sigma_{\text{GF}} \propto |\kappa_t + \kappa_g|^2$. Therefore, low energy measurements, such as on-shell and non-boosted Higgs production [13, 15, 40–46], are unable to resolve the $|\kappa_t + \kappa_g| = \text{constant}$ degeneracy. While the combination between the $t\bar{t}H$ and gluon fusion Higgs production have the potential to break this blind direction [47], we will illustrate that the Higgs production at the off-shell regime can also result into relevant contributions to resolve this degeneracy.

Since the Higgs boson decays mostly to longitudinal gauge bosons at the high energy regime, it is enlightening to inspect the signal amplitude for the longitudinal components. The amplitudes associated to each contribution presented in Fig. 5 can be approximated at

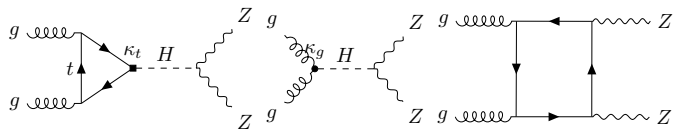


Figure 5. Feynman diagrams for the GF $gg \rightarrow ZZ$ process. The new physics effects from Eq. (6) display deviations on the coefficients κ_t and κ_g from the SM point $(\kappa_t, \kappa_g) = (1, 0)$.

$m_{ZZ} \gg m_t, m_H, m_Z$ by [13, 15, 48]

$$\begin{aligned} \mathcal{M}_t^{++00} &\approx + \frac{m_t^2}{2m_Z^2} \log^2 \frac{m_{ZZ}^2}{m_t^2}, \\ \mathcal{M}_g^{++00} &\approx - \frac{m_{ZZ}^2}{2m_Z^2}, \\ \mathcal{M}_c^{++00} &\approx - \frac{m_t^2}{2m_Z^2} \log^2 \frac{m_{ZZ}^2}{m_t^2}. \end{aligned} \quad (7)$$

Two comments are in order. First, both the s -channel top loop \mathcal{M}_t and the continuum \mathcal{M}_c amplitudes display logarithmic dependences on m_{ZZ}/m_t at the far off-shell regime. In the SM scenario the ultraviolet logarithm between these two amplitudes cancel, ensuring a proper high energy behavior when calculating the full amplitude. Second, it is worth noting the difference in sign between the s -channel contributions \mathcal{M}_t and \mathcal{M}_g . This results into a destructive interference between \mathcal{M}_t and \mathcal{M}_c , contrasting to a constructive interference between

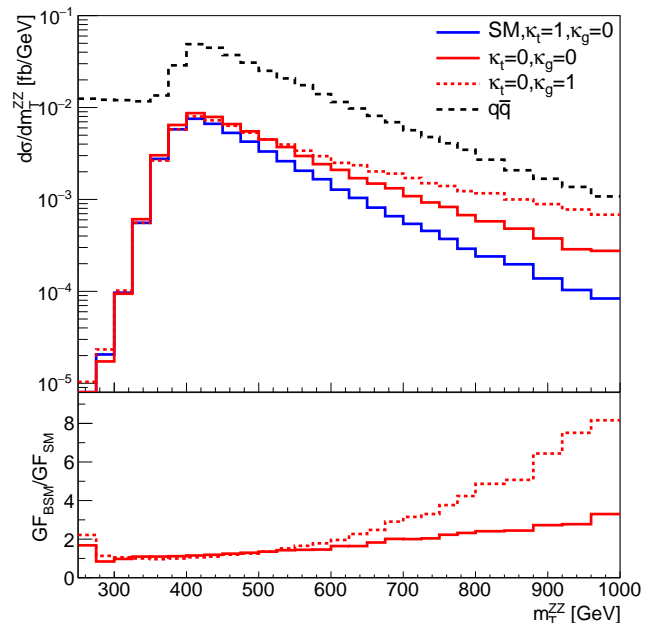


Figure 6. Transverse mass distributions m_T^{ZZ} for the DY and GF $Z(\ell\ell)Z(\nu\nu)$ processes. The new physics effects are parametrized by deviations from SM point $(\kappa_t, \kappa_g) = (1, 0)$. We follow the benchmark analysis defined in Sec II.

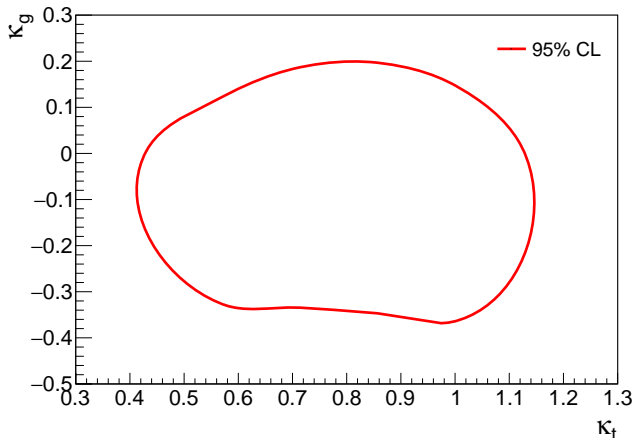


Figure 7. 95% CL bound on the coupling modifiers κ_t and κ_g when accounting for the off-shell Higgs measurement in the $Z(\ell\ell)Z(\nu\nu)$ channel. We assume the 14 TeV LHC with 3 ab^{-1} of data.

\mathcal{M}_g and \mathcal{M}_c . In the following, we will explore these phenomenological effects pinning down the new physics sensitivity with a higher precision.

Exploiting the larger rate for $ZZ \rightarrow \ell\ell\nu\nu$ than that for $ZZ \rightarrow 4\ell$ [13–15], we explore the off-shell Higgs physics at the HL-LHC. To simulate the full loop-induced effects, we implemented Eq. (6) into FeynRules/NLOCT [49, 50] through a new fermion state, and adjusting its parameters to match the low-energy Higgs interaction $HG_{\mu\nu}G^{\mu\nu}$ [38, 39]. Feynman rules are exported to a Universal FeynRules Output (UFO) [51] and the Monte Carlo event generation is performed with MadGraph5aMC@NLO [20].

In Fig. 6, we present the Drell-Yan (DY) and the gluon-fusion (GF) m_T^{ZZ} distributions for different signal hypotheses. In the bottom panel, we display the ratio between the GF beyond the SM (BSM) scenarios with respect to the GF SM. In agreement with Eq. (7), we observe a suppression for the full process when accounting for the s -channel top loop contributions and an enhancement when including the new physics terms associated to \mathcal{M}_g at high energies.

We follow the benchmark analysis defined in Sec. II. After the BDT study, the resulting events are used in a binned log-likelihood analysis with the m_T^{ZZ} distribution. This approach explores the characteristic high energy behavior for the new physics terms highlighted in Eq. (7) and illustrated in Fig. 6. We present in Fig. 7 the resulting 95% CL sensitivity to the (κ_t, κ_g) new physics parameters at the high-luminosity LHC. In particular, we observe that the LHC can bound the top Yukawa within $\kappa_t \approx [0.4, 1.1]$ at 95% CL, using this single off-shell channel. The observed asymmetry in the limit, in respect to the SM point, arises from the large and negative interference term between the s -channel and the continuum amplitudes. The upper bound on κ_t is complementary to the direct Yukawa measurement via $t\bar{t}H$ [52] and can be

further improved through a combination with the additional relevant off-shell Higgs final states. The results derived in this section are competitive to the CMS HL-LHC prediction that considers the boosted Higgs production combining the $H \rightarrow 4\ell$ and $H \rightarrow \gamma\gamma$ channels [34]. The CMS projection results into an upper bound on the top Yukawa of $\kappa_t \lesssim 1.2$ at 95% CL.

IV. HIGGS-TOP FORM FACTOR

The fact that the observed Higgs boson mass is much lighter than the Planck scale implies that there is an unnatural cancellation between the bare mass and the quantum corrections. Since the mass of the Higgs particle is not protected from quantum corrections, it is well-motivated to consider that it may not be fundamental, but composite in nature [53–56]. In such a scenario, the Higgs boson is proposed as a bound state of a strongly interacting sector with a composite scale Λ . In addition, the top quark, which is the heaviest particle in the SM, can also be composite. In this case, the top Yukawa coupling will be modified by a momentum-dependent form factor at a scale q^2 close to or above the new physics scale Λ^2 . It is challenging to find a general construction for such form factor without knowing the underlying dynamics. Here, we will adopt a phenomenological ansatz motivated by the nucleon form factor [57]. It is defined

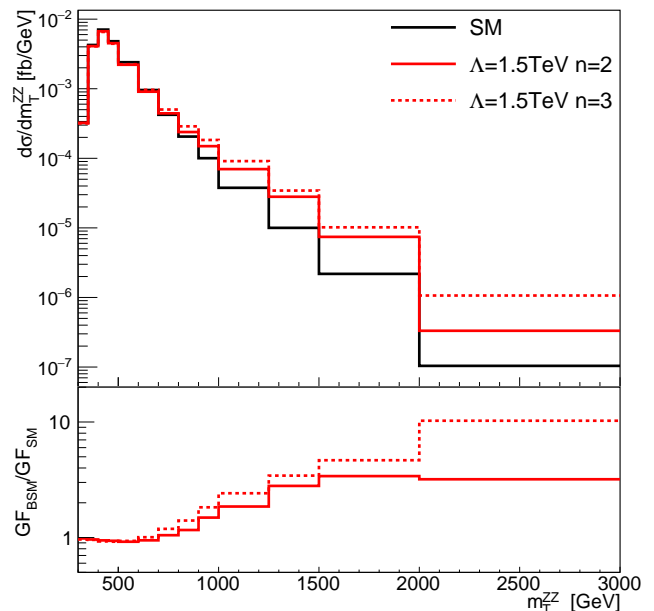


Figure 8. Transverse mass distribution m_T^{ZZ} for $gg(\rightarrow H^*) \rightarrow Z(2\ell)Z(2\nu)$ in the Standard Model (black) and with a new physics form factor (red). We assume $n = 2, 3$ and $\Lambda = 1.5 \text{ TeV}$ for the form factor scenario.

	Γ_H/Γ_H^{SM}	Λ_{EFT}	$\Lambda_{Composite}^{n=2}$
$H^* \rightarrow ZZ \rightarrow \ell\nu\nu$	1.31	0.8 TeV	1.5 TeV
$H^* \rightarrow ZZ \rightarrow 4\ell$	1.3 (68% CL) [33]	0.55 TeV [34]	0.8 TeV [18]

Table I. Comparison of the sensitivity reaches between $H^* \rightarrow ZZ \rightarrow \ell\nu\nu$ in this study and $H^* \rightarrow ZZ \rightarrow 4\ell$ in the literature as quoted. All results are presented at 95% CL except for the Higgs width projection derived by ATLAS with 68% CL [33]. We assume that the Wilson coefficient for the EFT framework is given by $c_t = v^2/\Lambda_{EFT}^2$. Besides the $H \rightarrow 4\ell$ channel, Ref. [34] also accounts for the $H \rightarrow \gamma\gamma$ final state with a boosted Higgs analysis.

as

$$\Gamma(q^2/\Lambda^2) = \frac{1}{(1 + q^2/\Lambda^2)^n}, \quad (8)$$

where q^2 is the virtuality of the Higgs boson. For $n = 2$, it is a dipole-form factor and corresponds to an exponential spacial distribution. Building upon Ref. [18], we study the impact of this form factor on $gg \rightarrow H^* \rightarrow ZZ$ process now with the complementary final state $\ell^+\ell^-\nu\bar{\nu}$.

In Fig. 8, we illustrate the m_T^{ZZ} distribution for the full gluon fusion $gg(\rightarrow H^*) \rightarrow ZZ$ process. We show the Standard Model (black) and the form factor scenario (red). We assume $n = 2$ or 3 and $\Lambda = 1.5$ TeV for the depicted form factor scenarios. The differences between Standard Model and form factor cases become larger when the energy scales are comparable or above Λ due to the suppression of destructive interference between Higgs signal and continuum background. Thus, we perform the same BDT procedure introduced in Sec. II followed by a binned log-likelihood ratio test in the m_T^{ZZ} distribution to fully explore this effect. In Fig. 9, we display the sensitivity reach for the LHC in the Higgs-top form factor. We observe that the LHC can bound these new physics effects up to $\Lambda = 1.5$ TeV for $n = 2$ and $\Lambda = 2.1$ TeV for $n = 3$ at 95% CL. The large event rate for the $H^* \rightarrow ZZ \rightarrow \ell\nu\nu$ signal results in a more precise probe to the ultraviolet regime than for the $H^* \rightarrow ZZ \rightarrow 4\ell$ channel, where the

limits on the new physics scale are $\Lambda = 0.8$ TeV for $n = 2$ and $\Lambda = 1.1$ TeV for $n = 3$ at 95% CL [18].

V. SUMMARY

We have systematically studied the off-shell Higgs production in the $pp \rightarrow H^* \rightarrow Z(\ell\ell)Z(\nu\nu)$ channel at the high-luminosity LHC. We showed that this signature is crucial to probe the Higgs couplings across different energy scales potentially shedding light on new physics at the ultraviolet regime. To illustrate its physics potential, we derived the LHC sensitivity to three BSM benchmark scenarios where the new physics effects are parametrized in terms of the Higgs boson width, the effective field theory framework, and a non-local Higgs-top coupling form factor.

The combination of a large signal rate and a precise phenomenological probe for the process energy scale, due to the transverse ZZ mass, renders strong limits for all considered BSM scenarios. A summary table and comparison with the existing results in the literature are provided in Table I. Adopting Machine-learning techniques, we demonstrated in the form of BDT that the HL-LHC, with $\mathcal{L} = 3 \text{ ab}^{-1}$ of data, will display large sensitivity to the Higgs boson width, $\Gamma_H/\Gamma_H^{SM} < 1.31$. In addition, the characteristic high energy behavior for the new physics terms within the EFT framework results in relevant bounds on the (κ_t, κ_g) new physics parameters, resolving the low energy degeneracy in the gluon fusion Higgs production. In particular, we observe that the LHC can bound the top Yukawa within $\kappa_t \approx [0.4, 1.1]$ at 95% CL. The upper bound on κ_t is complementary to the direct Yukawa measurement via $t\bar{t}H$ and can be further improved in conjunction with additional relevant off-shell Higgs channels. Finally, when considering a more general hypothesis that features a non-local momentum-dependent Higgs-top interaction, we obtain that the HL-LHC is sensitive to new physics effects at large energies with $\Lambda = 1.5$ TeV for $n = 2$ and $\Lambda = 2.1$ TeV for $n = 3$ at 95% CL. We conclude that, utilizing the promising $H^* \rightarrow Z(\ell^+\ell^-)Z(\nu\bar{\nu})$ channel at the HL-LHC and adopting the Machine-Learning techniques, the combination of a large signal rate and a precise phenomenological probe for the process energy scale renders improved sensitivities beyond the existing literature, to all the three BSM scenarios considered in this work.

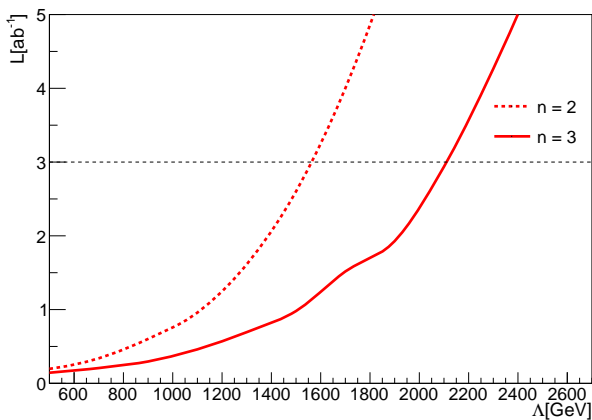


Figure 9. 95% CL sensitivity on the new physics scale Λ as a function of the LHC luminosity. We assume the form factor in Eq. (8) with $n = 2$ (dashed line) and $n = 3$ (solid line) at the 14 TeV LHC.

ACKNOWLEDGMENTS

This work was supported by the U.S. Department of Energy under grant No. DE-FG02-95ER40896 and by

the PITT PACC. DG was supported by the U.S. Department of Energy under grant number DE-SC 0016013.

-
- [1] Peter W. Higgs. Broken symmetries, massless particles and gauge fields. *Phys. Lett.*, 12:132–133, 1964.
- [2] Peter W. Higgs. Broken symmetries and the masses of gauge bosons. *Phys. Rev. Lett.*, 13:508–509, Oct 1964.
- [3] F. Englert and R. Brout. Broken symmetry and the mass of gauge vector mesons. *Phys. Rev. Lett.*, 13:321–323, Aug 1964.
- [4] G. Aad, T. Abajyan, B. Abbott, J. Abdallah, S. Abdel Khalek, A.A. Abdelalim, O. Abdinov, R. Aben, B. Abi, M. Abolins, and et al. Observation of a new particle in the search for the standard model higgs boson with the atlas detector at the lhc. *Physics Letters B*, 716(1):1–29, Sep 2012.
- [5] S. Chatrchyan, V. Khachatryan, A.M. Sirunyan, A. Tumasyan, W. Adam, E. Aguilo, T. Bergauer, M. Dragicevic, J. Erö, C. Fabjan, and et al. Observation of a new boson at a mass of 125 gev with the cms experiment at the lhc. *Physics Letters B*, 716(1):30–61, Sep 2012.
- [6] Nikolas Kauer and Giampiero Passarino. Inadequacy of zero-width approximation for a light Higgs boson signal. *JHEP*, 08:116, 2012.
- [7] Fabrizio Caola and Kirill Melnikov. Constraining the Higgs boson width with ZZ production at the LHC. *Phys. Rev.*, D88:054024, 2013.
- [8] John M. Campbell, R. Keith Ellis, and Ciaran Williams. Bounding the Higgs width at the LHC using full analytic results for $gg \rightarrow e^- e^+ \mu^- \mu^+$. *JHEP*, 04:060, 2014.
- [9] Morad Aaboud et al. Constraints on off-shell Higgs boson production and the Higgs boson total width in $ZZ \rightarrow 4\ell$ and $ZZ \rightarrow 2\ell 2\nu$ final states with the ATLAS detector. *Phys. Lett. B*, 786:223–244, 2018.
- [10] Albert M Sirunyan et al. Measurements of the Higgs boson width and anomalous HVV couplings from on-shell and off-shell production in the four-lepton final state. *Phys. Rev. D*, 99(11):112003, 2019.
- [11] James S. Gainer, Joseph Lykken, Konstantin T. Matchev, Stephen Mrenna, and Myeonghun Park. Beyond Geolocating: Constraining Higher Dimensional Operators in $H \rightarrow 4\ell$ with Off-Shell Production and More. *Phys. Rev. D*, 91(3):035011, 2015.
- [12] Giacomo Cacciapaglia, Aldo Deandrea, Guillaume Drieu La Rochelle, and Jean-Baptiste Flament. Higgs couplings: disentangling New Physics with off-shell measurements. *Phys. Rev. Lett.*, 113(20):201802, 2014.
- [13] Aleksandr Azatov, Christophe Grojean, Ayan Paul, and Ennio Salvioni. Taming the off-shell Higgs boson. *Zh. Eksp. Teor. Fiz.*, 147:410–425, 2015.
- [14] Christoph Englert and Michael Spannowsky. Limitations and Opportunities of Off-Shell Coupling Measurements. *Phys. Rev. D*, 90:053003, 2014.
- [15] Malte Buschmann, Dorival Goncalves, Silvan Kuttimalai, Marek Schonherr, Frank Krauss, and Tilman Plehn. Mass Effects in the Higgs-Gluon Coupling: Boosted vs Off-Shell Production. *JHEP*, 02:038, 2015.
- [16] Tyler Corbett, Oscar J. P. Eboli, Dorival Goncalves, J. Gonzalez-Fraile, Tilman Plehn, and Michael Rauch. The Higgs Legacy of the LHC Run I. *JHEP*, 08:156, 2015.
- [17] Dorival Goncalves, Tao Han, and Satyanarayan Mukhopadhyay. Off-Shell Higgs Probe of Naturalness. *Phys. Rev. Lett.*, 120(11):111801, 2018. [Erratum: *Phys.Rev.Lett.* 121, 079902 (2018)].
- [18] Dorival Goncalves, Tao Han, and Satyanarayan Mukhopadhyay. Higgs Couplings at High Scales. *Phys. Rev.*, D98(1):015023, 2018.
- [19] Christoph Englert, Yotam Soreq, and Michael Spannowsky. Off-Shell Higgs Coupling Measurements in BSM scenarios. *JHEP*, 05:145, 2015.
- [20] J. Alwall, R. Frederix, S. Frixione, V. Hirschi, F. Maltoni, O. Mattelaer, H. S. Shao, T. Stelzer, P. Torrielli, and M. Zaro. The automated computation of tree-level and next-to-leading order differential cross sections, and their matching to parton shower simulations. *JHEP*, 07:079, 2014.
- [21] Valentin Hirschi and Olivier Mattelaer. Automated event generation for loop-induced processes. *JHEP*, 10:146, 2015.
- [22] Stefano Frixione and Bryan R. Webber. Matching NLO QCD computations and parton shower simulations. *JHEP*, 06:029, 2002.
- [23] Marco Bonvini, Fabrizio Caola, Stefano Forte, Kirill Melnikov, and Giovanni Ridolfi. Signal-background interference effects for $gg \rightarrow H \rightarrow W^+ W^-$ beyond leading order. *Phys. Rev.*, D88(3):034032, 2013.
- [24] Pierre Artoisenet, Rikkert Frederix, Olivier Mattelaer, and Robbert Rietkerk. Automatic spin-entangled decays of heavy resonances in Monte Carlo simulations. *JHEP*, 03:015, 2013.
- [25] Richard D. Ball, Valerio Bertone, Stefano Carrazza, Luigi Del Debbio, Stefano Forte, Alberto Guffanti, Nathan P. Hartland, and Juan Rojo. Parton distributions with QED corrections. *Nucl. Phys.*, B877:290–320, 2013.
- [26] Torbjörn Sjöstrand, Stefan Ask, Jesper R. Christiansen, Richard Corke, Nishita Desai, Philip Ilten, Stephen Mrenna, Stefan Prestel, Christine O. Rasmussen, and Peter Z. Skands. An Introduction to PYTHIA 8.2. *Comput. Phys. Commun.*, 191:159–177, 2015.
- [27] S. Ovin, X. Rouby, and V. Lemaitre. DELPHES, a framework for fast simulation of a generic collider experiment. 2009.
- [28] Andreas Hoecker, Peter Speckmayer, Joerg Stelzer, Jan Therhaag, Eckhard von Toerne, and Helge Voss. TMVA: Toolkit for Multivariate Data Analysis. *PoS, ACAT:040*, 2007.
- [29] Dorival Goncalves and Junya Nakamura. Role of the Z polarization in the $H \rightarrow b\bar{b}$ measurement. *Phys. Rev.*, D98(9):093005, 2018.
- [30] Dorival Goncalves and Junya Nakamura. Boosting the $H \rightarrow$ invisibles searches with Z boson polarization. *Phys. Rev.*, D99(5):055021, 2019.

- [31] John C. Collins and Davison E. Soper. Angular Distribution of Dileptons in High-Energy Hadron Collisions. *Phys. Rev.*, D16:2219, 1977.
- [32] Dorival Goncalves, Tilman Plehn, and Jennifer M. Thompson. Weak boson fusion at 100 TeV. *Phys. Rev.*, D95(9):095011, 2017.
- [33] Off-shell Higgs boson couplings measurement using $H \rightarrow ZZ \rightarrow 4l$ events at High Luminosity LHC. 2015.
- [34] Sensitivity projections for Higgs boson properties measurements at the HL-LHC. 11 2018.
- [35] Thomas Appelquist and J. Carazzone. Infrared Singularities and Massive Fields. *Phys. Rev. D*, 11:2856, 1975.
- [36] W. Buchmuller and D. Wyler. Effective Lagrangian Analysis of New Interactions and Flavor Conservation. *Nucl. Phys. B*, 268:621–653, 1986.
- [37] B. Grzadkowski, M. Iskrzynski, M. Misiak, and J. Rosiek. Dimension-Six Terms in the Standard Model Lagrangian. *JHEP*, 10:085, 2010.
- [38] Mikhail A. Shifman, A.I. Vainshtein, M.B. Voloshin, and Valentin I. Zakharov. Low-Energy Theorems for Higgs Boson Couplings to Photons. *Sov. J. Nucl. Phys.*, 30:711–716, 1979.
- [39] Bernd A. Kniehl and Michael Spira. Low-energy theorems in Higgs physics. *Z. Phys. C*, 69:77–88, 1995.
- [40] U. Baur and E.W.Nigel Glover. Higgs Boson Production at Large Transverse Momentum in Hadronic Collisions. *Nucl. Phys. B*, 339:38–66, 1990.
- [41] Robert V. Harlander and Tobias Neumann. Probing the nature of the Higgs-gluon coupling. *Phys. Rev. D*, 88:074015, 2013.
- [42] Andrea Banfi, Adam Martin, and Veronica Sanz. Probing top-partners in Higgs+jets. *JHEP*, 08:053, 2014.
- [43] Aleksandr Azatov and Ayan Paul. Probing Higgs couplings with high p_T Higgs production. *JHEP*, 01:014, 2014.
- [44] Christophe Grojean, Ennio Salvioni, Matthias Schlaffer, and Andreas Weiler. Very boosted Higgs in gluon fusion. *JHEP*, 05:022, 2014.
- [45] Malte Buschmann, Christoph Englert, Dorival Goncalves, Tilman Plehn, and Michael Spannowsky. Resolving the Higgs-Gluon Coupling with Jets. *Phys. Rev. D*, 90(1):013010, 2014.
- [46] Aleksandr Azatov, Christophe Grojean, Ayan Paul, and Ennio Salvioni. Resolving gluon fusion loops at current and future hadron colliders. *JHEP*, 09:123, 2016.
- [47] Michelangelo L. Mangano, Tilman Plehn, Peter Reimitz, Torben Schell, and Hua-Sheng Shao. Measuring the Top Yukawa Coupling at 100 TeV. *J. Phys. G*, 43(3):035001, 2016.
- [48] E.W.Nigel Glover and J.J. van der Bij. Z BOSON PAIR PRODUCTION VIA GLUON FUSION. *Nucl. Phys. B*, 321:561–590, 1989.
- [49] Adam Alloul, Neil D. Christensen, Céline Degrande, Claude Duhr, and Benjamin Fuks. FeynRules 2.0 - A complete toolbox for tree-level phenomenology. *Comput. Phys. Commun.*, 185:2250–2300, 2014.
- [50] Céline Degrande. Automatic evaluation of UV and R2 terms for beyond the Standard Model Lagrangians: a proof-of-principle. *Comput. Phys. Commun.*, 197:239–262, 2015.
- [51] Céline Degrande, Claude Duhr, Benjamin Fuks, David Grellscheid, Olivier Mattelaer, and Thomas Reiter. Ufo – the universal feynrules output. *Computer Physics Communications*, 183(6):1201–1214, Jun 2012.
- [52] M. Cepeda et al. Report from Working Group 2: Higgs Physics at the HL-LHC and HE-LHC. *CERN Yellow Rep. Monogr.*, 7:221–584, 2019.
- [53] Alex Pomarol and Francesco Riva. The Composite Higgs and Light Resonance Connection. *JHEP*, 08:135, 2012.
- [54] Giuliano Panico and Andrea Wulzer. The Discrete Composite Higgs Model. *JHEP*, 09:135, 2011.
- [55] Giuliano Panico and Andrea Wulzer. The Composite Nambu-Goldstone Higgs. *Lect. Notes Phys.*, 913:pp.1–316, 2016.
- [56] Da Liu, Ian Low, and Carlos E. M. Wagner. Modification of Higgs Couplings in Minimal Composite Models. *Phys. Rev.*, D96(3):035013, 2017.
- [57] V. Punjabi, C. F. Perdrisat, M. K. Jones, E. J. Brash, and C. E. Carlson. The Structure of the Nucleon: Elastic Electromagnetic Form Factors. *Eur. Phys. J.*, A51:79, 2015.